Supplemental Methods

Study design, IRB and ethical considerations

The UK Biobank is a phenotyped, prospective, population-based cohort of 500,000 individuals between the ages of 40-69 recruited by mail from 2006-2010[1]. Within the UK Biobank, some 100,000 individuals underwent cardiac magnetic resonance (CMR) imaging[2, 3]. Cardiac magnetic resonance imaging was performed with 1.5 Tesla scanners (MAGNETOM Aera, Siemens Healthcare), using electrocardiographic gating for cardiac synchronization[3]. In total, quality control measures detailed in our previous work suggest that in this study, 2.3 million images from 45,000 individuals would be eligible for analysis[4]. UK Biobank access is provided under application 7089. Analysis is approved by the Mass General Brigham institutional review board (protocol 2003P001563). Identifiers of UK Biobank subjects who have withdrawn consent since the time of their enrollment are regularly distributed by the repository; these subjects are excluded from future analyses.

Annotation

Segmentation maps of the cine images have been traced manually (MN) as supervised by a cardiologist (JPP). In our prior work we noted that a similar downstream deep learning model for CMR images produced optimum downstream pixel accuracy when trained with at least 116 manually annotated images, and that additional accuracy gleaned from training with up to 500 manually annotated images was modest[4]. Thus, in the present work 250 samples were chosen at random, manually segmented, and then used to train a deep learning model with fastai v1.0.5945[5]. The model was U-net derived with an encoder pre-trained on ImageNet to optimize for the recognition of natural shapes[6, 7]. Training and validation subsets comprised 80% and 20% of the samples, respectively. The training model was found to achieve 99.8% pixel

segmentation accuracy (Jaccard agreement 84.3%) for annotation of the LVOT in the held-out validation set. Pulmonary artery segmentation was used as a secondary annotation metric; for this structure the pixel segmentation accuracy was found to be 99.9% (Jaccard agreement 87.3%).

Calculation of diameters of anatomic structures

The LVOT, the aortic root, and the ascending aorta, are captured in the long axis of the contiguous tract they form. As annotated in this plane, the LVOT, aortic root, and proximal part of the ascending aorta often appear to be rectangular. To extract their diameters, first, the centerline of the contiguous tract formed by the LV cavity, LVOT, aortic root, and ascending aorta was calculated using the algorithm skeletonize implemented by the image processing package scikit-image[8, 9]. Orthogonal measurements to the tract centerline were taken at the respective centroids of the LVOT and aortic root complex. These normal lines were then intersected with the boundaries of the respective structure to give two coordinates representing the bounds of the diameter measurements. The Euclidean distance between the diameter boundaries, converted from pixels to millimeters based on image metadata, represented the diameters of the LVOT and aortic root (**Figure 1**).

For the ascending aorta, rather than a single diameter taken at the centroid, we took several diameters that we sought to align between participants to represent similar levels of aorta. To achieve this, we used height as a proxy for aorta length. We defined the centerline at the border with the sinotubular junction as a reference point. We then identified the point on the centerline 3 mm distal to this border, and via a perpendicular line as for the proximal structures, measured a diameter at this point ("Aorta 0"). We then took subsequent diameters of the aorta at intervals of 10 mm multiplied by the ratio of the participant's height to the mean height of the dataset (i.e.

169 cm). For example, a participant of mean height would have diameters of the aorta taken, starting at the border with the aortic root, at 3 mm, 13 mm, 23 mm, and so on (see **Supplemental Table 5** for descriptions of all phenotypes). These measurements are taken closer together for a shorter-than-average participant and farther apart for a taller-than-average participant. Because a variable length of aorta was visualized across participants (and across studies) because of variation in its orientation relative to the imaging plane, the number of ascending aorta diameters that we could measure for each participant was, similarly, variable.

Quality control of image segmentation and phenotype extraction

Images were filtered to those containing one component for each of: left ventricle cavity, LVOT, and aortic root. Images containing an LV cavity of less than 100 pixels were discarded due to biologic implausibility. Phenotypic measurements of LVOT diameter, aortic root diameter, or ascending aorta diameter at any level less than 1cm were discarded due to biologic implausibility. If a given participant was imaged on multiple occasions, we kept only the first study in order to facilitate comparisons with prior published work. It was observed that greater than 50% of the participants in the dataset had measurements of the aorta at levels Aorta 0 through Aorta 5. More distal levels were thus excluded due to incompleteness.

We observed that the contiguous tract of LVOT, aortic root, and ascending aorta were most often captured in correct planar arrangement at the beginning of the MRI CINE: a point of the cardiac cycle corresponding to left ventricular end-diastole. Other points of the cardiac cycle, for example ventricular end-systole, failed to capture the aorta in-plane. Therefore, for a given MRI study, we chose the first frame for subsequent analysis, or the second frame if the first frame had failed upstream QC. We confirmed that the mean LV cavity size using this approach very closely approximated the corresponding value if instead the maximum LV cavity for each participant

were chosen. We thus concluded that choosing the first or second frame of the study appropriately maximized the likelihood of a correct planar arrangement while remaining very close to true ventricular end-diastole.

To identify any remaining images with an incorrect planar arrangement, we exploited the fact that we have previously measured the diameter of the ascending aorta in its cross section (short axis) using a different deep learning model trained by different operators[4]. We compared the present work's estimates of structure diameters against the previously published diameters of ascending aorta in its short axis. We found that the LVOT-view-derived diameters for ascending aorta at position Aorta 2 correlated most strongly with the previously published phenotype (Pearson's r = 0.83). We then investigated the ratio of LVOT-view-derived diameters to the previously published short axis diameter and found that the ratio closely approached parity at aorta position 2 (median = 0.98, interquartile range = 0.08). As such, we hypothesized that the previously investigated short axis plane was likely taken most often nearest to the position labeled Aorta 2 in our present study. As discussed in **Supplemental Methods: Calculation of diameters of anatomic structures**, this point corresponds to approximately 23 mm distal to the border with the aortic root for a participant of average height.

We further hypothesized that points for which the relationship between the LVOT-view-derived diameter Aorta 2 and the short axis diameter of the aorta diverges significantly from a linear relationship represent out-of-plane images. We thus constructed a linear model relating these two phenotypes and obtained 99% prediction intervals for all values of the independent variable: ascending aorta taken from the LVOT view at position 2. Those points with a corresponding ascending aorta diameter derived from its short axis view fell outside the 99% prediction intervals were discarded. To avoid accidentally yielding signals of known disease, we excluded

participants with prevalent atrial fibrillation, heart failure, myocardial infarction, or coronary artery disease prior to MRI (n = 1948, 5% of the pre-exclusion group). We finally excluded participants with lack of genetic data, sample QC missing rate greater than or equal to 2%, sex chromosome aneuyploidy, or outlier status for heterozygosity (n = 1452, 4% of the pre-exclusion group) (**Supplemental Figure 1**). After final quality control, up to 33,870 participants remained to be included in a GWAS; sample size decreased for GWAS traits of more distal ascending aorta given its variable visualization (**Supplemental Table 3**).

Genotyping and genome-wide association studies

Genotype information was obtained using either the UK BiLEVE or UK Biobank Axiom arrays; they were then imputed into the Haplotype Reference Consortium panel and the UK10K+1000 Genomes panel[10]. Participants were filtered to exclude those without imputed genetic data and those with a genotypic call rate < 0.98. Heritability values of structures of interest were then calculated using BOLT-REML on the genotyped variants in the UK Biobank[11]. Covariates included age at time of MRI, the first five principal components of ancestry, sex, the genotyping array, and the MRI scanner's unique identifier[12]. The latter covariate was included in this and other analyses to account for any potential differences in machine or image reconstruction variables between imaging sites.

Genome-wide association was tested using REGENIE 2.0.2, using the full autosomal panel of directly genotyped SNPs as the genetic relationship matrix and structure diameters as continuous phenotypes, as discussed[13]. GWAS covariates included age at time of MRI, the first five principal components of ancestry, sex, the genotyping array, and the MRI scanner's unique identifier[12]. The genome-wide significance threshold for SNPs was $P < 5\times10^{-8}$. To identify independently associated variants, linkage disequilibrium clumping was performed in the same

participants used to create the GWAS using plink-1.9 using a 5 megabase radius, an r^2 cutoff of 0.001, and the genome-wide P threshold[14]. For comparison of loci reaching genome-wide significance for multiple traits, a given locus was assigned a shared "global" locus identifying number with any other loci within 500 kilobases. Lead SNPs were tested for deviation from Hardy-Weinberg equilibrium (HWE) at the commonly-used threshold $P < 1x10^{-6}$. BOLT-REML v2.3.4 was used to assess the SNP heritability of all phenotypes[11].

Exome sequencing in UK Biobank

We conducted an exome sequencing analysis on over 200,000 exomes released by the UK Biobank. Samples from the UK Biobank were chosen for exome sequencing based on enrichment for MRI data and linked health records[15]. Exome sequencing was performed by Regeneron and reprocessed centrally by the UK Biobank following the Functional Equivalent pipeline[16]. Exomes were captured with the IDT xGen Exome Research Panel v1.0.The basic design targets 39Mbp of the human genome (19,396 genes). Multiplexed samples were sequenced with dual-indexed 75x75bp paired-end reads on the Illumina NovaSeq 6000 platform using S2 (first 50k samples) and S4 flow cells (subsequent 150k samples). Alignment to GRCh38 was performed in an alt-aware manner as described in the Functional Equivalence protocol. Individual level VCF files were combined and joint-genotyped using GLnexus after Variants were called per-sample using DeepVariant. We applied hard filters low-quality genotypes:

1. For homozygous reference calls: Genotype Quality < 20; Genotype Depth < 10; Genotype Depth > 200

2. For heterozygous calls: (A1 Depth + A2 Depth)/Total Depth < 0.9; A2 Depth/Total Depth < 0.2; Genotype likelihood[ref/ref] < 20; Genotype Depth < 10; Genotype Depth > 200
3. For homozygous alternative calls: (A1 Depth + A2 Depth)/Total Depth < 0.9; A2 Depth/Total Depth < 0.9; Genotype likelihood[ref/ref] < 20; Genotype Depth < 10; Genotype Depth > 200

Then, we performed variant level filters. Low-quality variants were removed followed by: Call rate < 90%, Hardy-Weinberg Equilibrium p-value < 10-15, present in Ensembel low-complexity regions, monomorphic variants in the final dataset. Finally, we calculated a few sample quality metrics and removed low-quality samples. Samples with withdrawn consent, sex mismatch, call rate < 90%, outliers (8 standard deviations apart from mean) of transition/transversion ratio, heterozygote/homozygote ratio, SNP/Indel ratio, and the number of singletons were removed. Variants were annotated with the Ensembl Variant Effect Predictor version 95 using the --pick-allele flag[17]. LOFTEE was used to identify high-confidence loss of function variants: stop-gain, splice-site disrupting, and frameshift variants[18]. To understand population-level frequencies of variants, we annotated 5 continental variant frequencies using gnomAD v2.

Rare variant association test

We conducted a collapsing burden test to assess the impact of loss-of-function variants in up to 18,461 participants who had measurements of diameters of interest and exome sequencing data available. Variants with MAF $\geq$ 0.001 or continental maximum MAF $\geq$ 0.001 were excluded. Using the LOFTEE "high-confidence" loss-of-function variants without a flag, we tested whether loss-of-function carrier status was associated with ascending aorta traits using the linear mixed-effect approach implemented in the R-package GENESIS. The model was adjusted for

age at MRI, sex, the MRI serial number, sequencing batch, associated PCs, and empirical kinship matrix. Protein-coding genes with the number of carriers <10 were removed from the results.

Comparison with prior work

We sought to compare our GWAS results with those of comparable studies. We identified one that investigated the genetics of ascending aorta diameter at a comparable anatomic location and one that investigated the genetics of aortic root diameter at a comparable anatomic location[4, 19]. To our knowledge, no prior study investigated the genetics of the LVOT diameter in a comparable way. For both aorta and aortic root, we deemed a trait novel if it was both (1) outside 500 kilobases from all SNPs in the prior work and (2) not in linkage disequilibrium with any SNP in the prior work. To query linkage disequilibrium we queried all SNPs with rsIDs against the associated prior work's SNPs using LDlink, specifying European populations to best match the UK Biobank participants and using an LD cutoff of $r^2 > 0.01$[20]. In one instance, LDlink was unable to resolve a SNP described in the present work (at chr5:15005465, associated with aortic root diameter). In this case we manually confirmed that there were no previously described SNPs in the associated prior work within 100 megabases.

Aortic disease codes

International Classification of Diseases version 10 (ICD-10) codes and Office of Population Censuses and Surveys Classification of Interventions and Procedures version 4 (OPCS-4) codes used to define diseases of interest are detailed in **Supplemental Table 1**. These definitions were used for GWAS participant exclusion and polygenic score assessment.

Trait-disease correlation

We sought to validate our diameters by investigating their correlations to prevalent disease (**Supplemental Table 6**). To do so we constructed linear models investigating the presence or

absence of a disease of interest as predicted by the inverse normal diameter of interest. Due to small available numbers of follow up (n = 12 for thoracic aortic aneurysm and n = 99 for aortic stenosis), these models are not adjusted for other covariates in order to avoid overfitting..

Association between polygenic risk scores and incident disease

Using PRScs (https://github.com/getian107/PRScs; git hash 43128be7fc9ca16ad8b85d8754c538bcfb7ec7b4), we computed polygenic risk scores for participants in the UK Biobank with genetic data available[21]. We computed a separate score using the GWAS of each described phenotype, using the autosomal, independently significant SNPs of the respective GWAS. We excluded participants whose data were used for the GWAS. We confirmed that polygenic scores were still well-correlated to their upstream traits by Pearson's r, despite the inverse normal transformation applied to traits prior to GWAS (Supplemental Table 7).

We analyzed the relationship between the resultant polygenic scores for individuals and several events using both unadjusted survival analyses and Cox proportional hazards models that were also adjusted for clinical risk factors. The events included incident thoracic aortic aneurysm (427,016 individuals, 743 events) and aortic stenosis (426,502 individuals, 3,604 events). There are limited data regarding clinical risk factors for thoracic aortic aneurysm outside of associated syndromes and family history, so we chose putatively relevant covariates based in part on inference from evidence in the abdominal aortic aneurysm literature[22]. These covariates included sex, body mass (the cubic natural spline of BMI), age (the cubic natural spline of age at enrollment, and its interaction with age), and blood pressure (the cubic natural splines of systolic and diastolic blood pressure measurements). We also adjusted for other covariates including the cubic natural spline of height, the cubic natural spline of weight, the genotyping array, and the

first five principal components of ancestry. This analysis was performed separately for each of the polygenic risk scores listed above. Proportional hazards violations were observed during modeling, so the results were confirmed with accelerated failure time models, which showed similar results (Supplemental Table 10). 47 participants were excluded from accelerated failure time models predicting aortic stenosis due to sub-year survival (1.3% of the original dataset, N_disease = 3551), which was felt unlikely to influence overall concordance of results with those of Cox proportional hazards.

Supplemental Figure 1: Quality control for GWAS

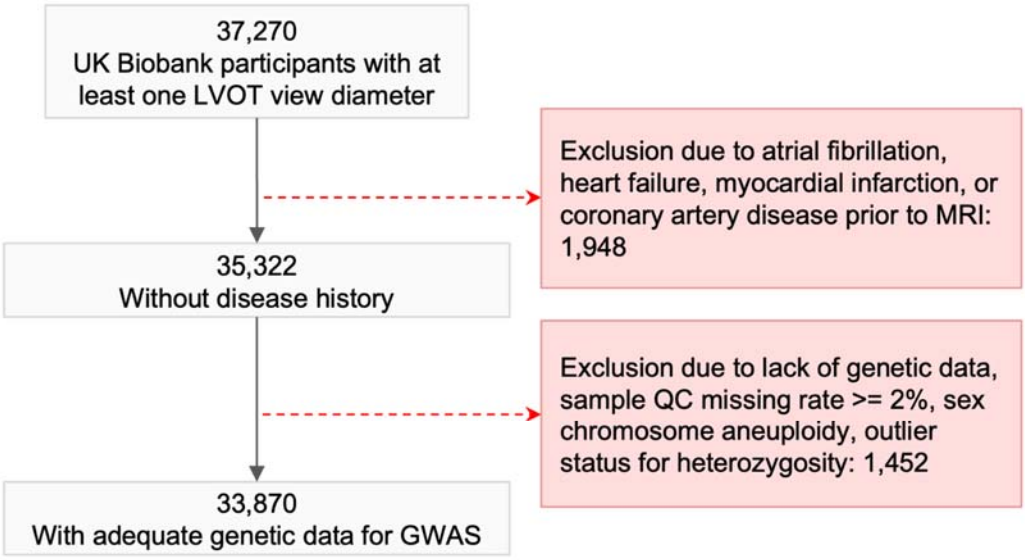

Supplemental Figure 2: Distributions of extracted diameters

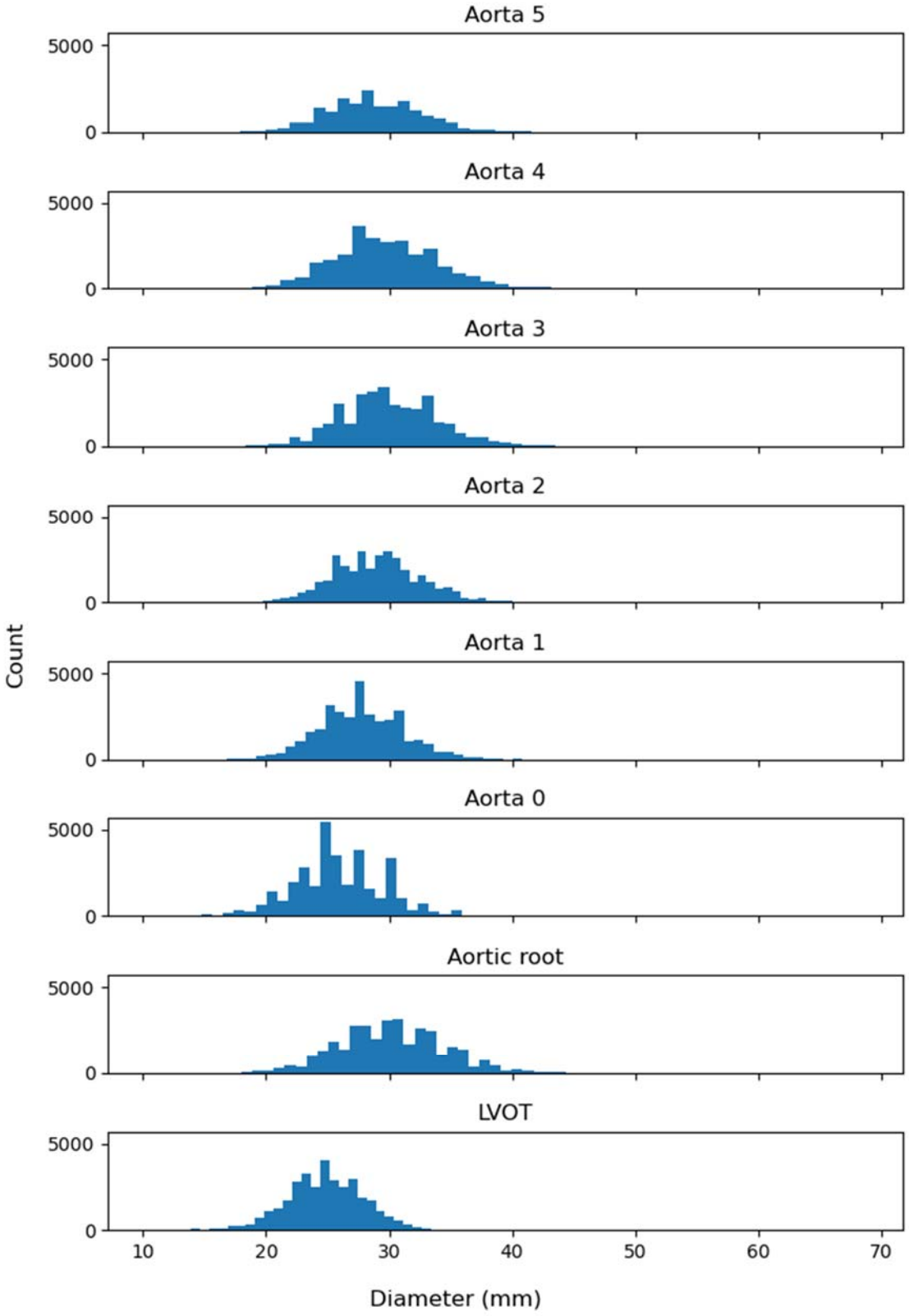

Supplemental Figure 3: Genetic correlations between inverse normal of traits

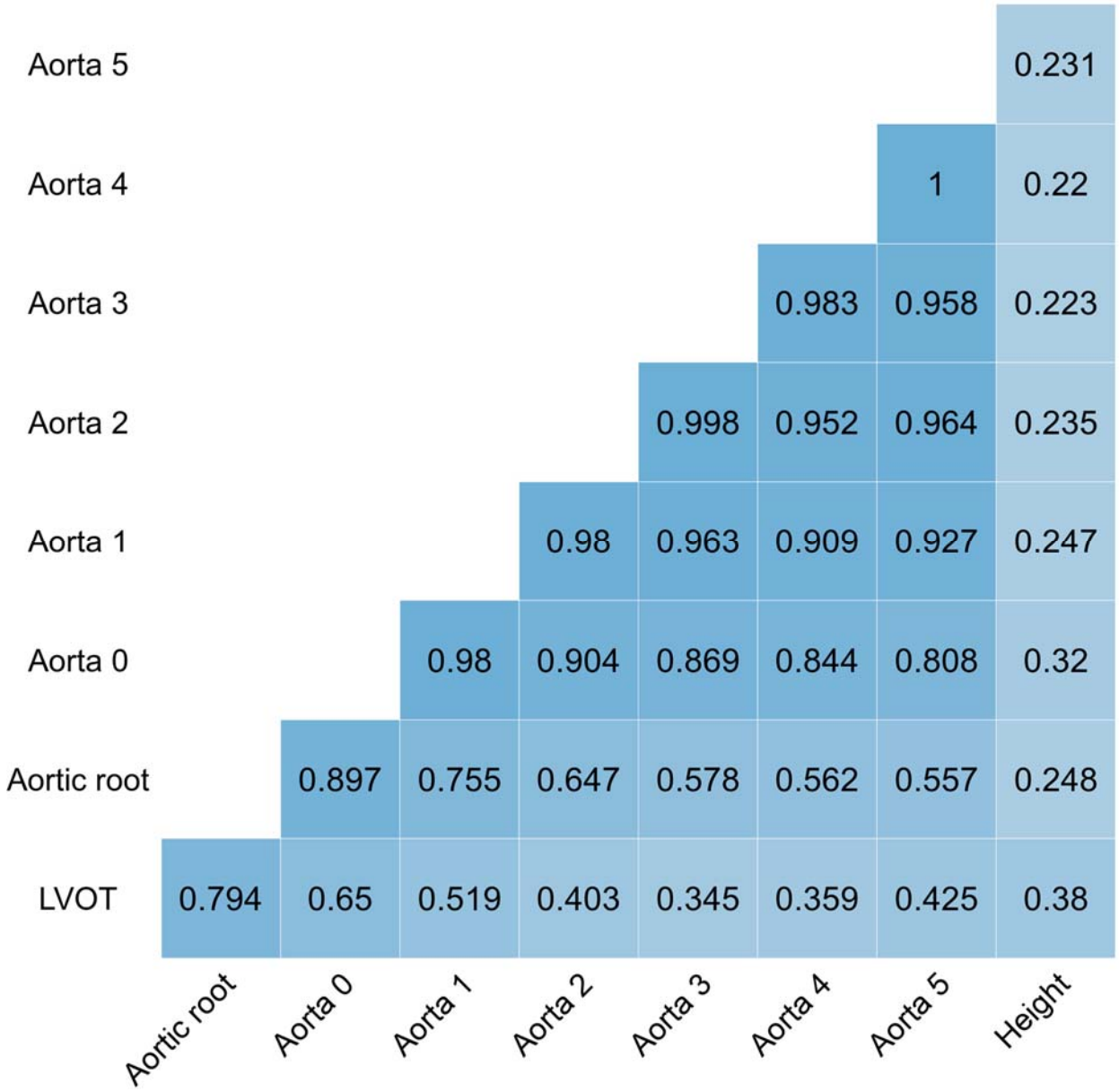

Supplemental Figure 4: Clustering of significant genetic associations

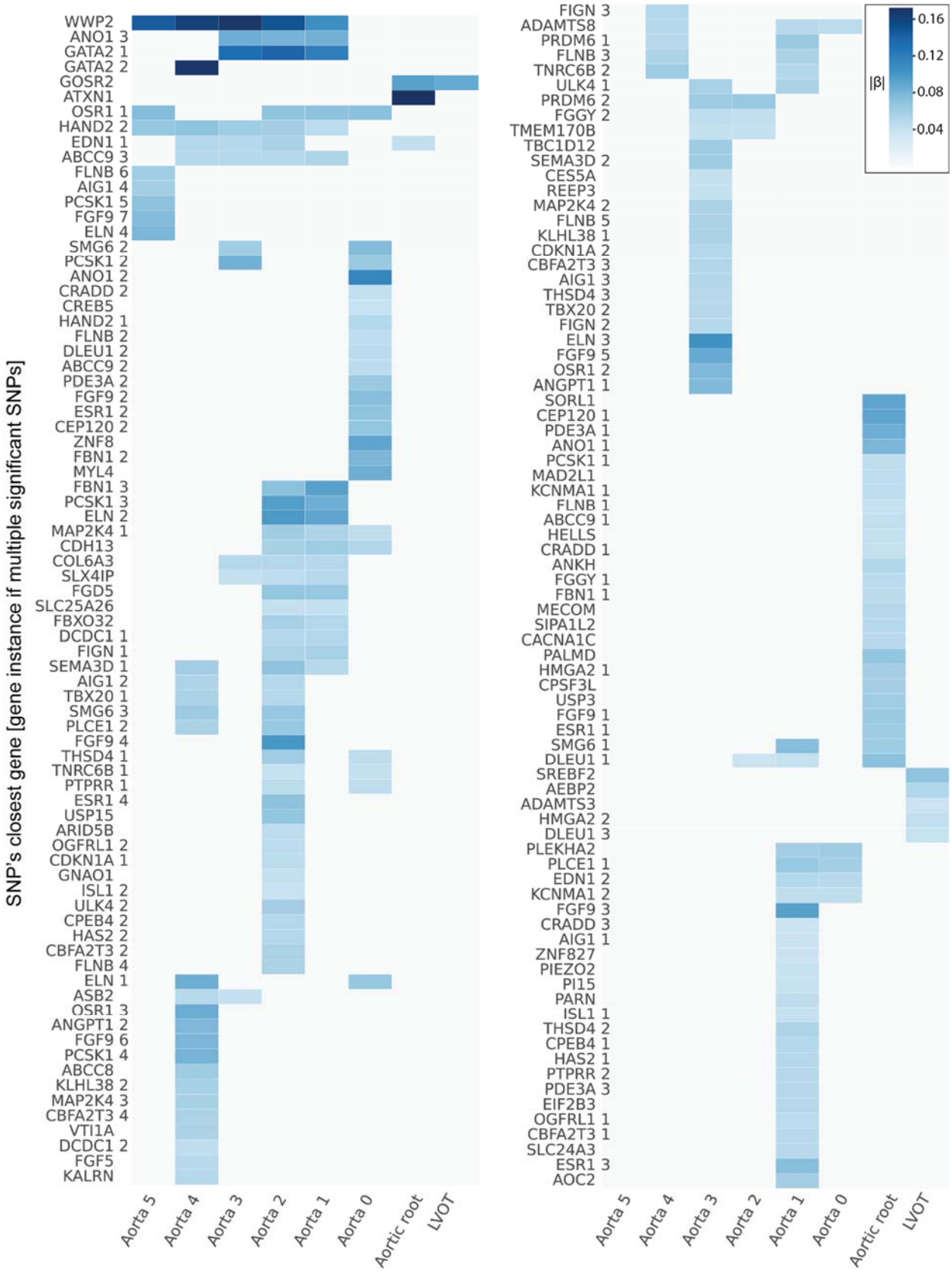

Column position denotes associated GWAS in fixed order. Rows denote SNPs associated with one or more traits at $P < 5x10^{-8}$. Row labels display genes nearest to associated SNPs. Where multiple SNPs share a closest gene, a number displays the gene's instance in the combined significant GWAS results. See Supplemental Table 8 for SNP names corresponding to row labels. Color indicates absolute effect size ($|\beta|$) per standard error of a SNP associated at $P < 5x10^{-8}$. To illustrate anatomic relationship of genome-wide significant SNPs, heatmap column position is hierarchically clustered to group SNP associations of similar significance (P). For this illustrative purpose, SNPs not meeting genome-wide significance are assigned P = 0.

Supplemental Table 1: Disease Codes

Pathology	**Definition [includes/ excludes] code**	**Code type**	**Diagnosis code**
Aortic stenosis	include	ICD10	I06.0 Rheumatic aortic stenosis
Aortic stenosis	include	ICD10	I06.2 Rheumatic aortic stenosis with insufficiency
Aortic stenosis	include	ICD10	I35.0 Aortic (valve) stenosis
Aortic stenosis	include	ICD10	I35.2 Aortic (valve) stenosis with insufficiency
Aortic stenosis	include	Non-cancer illness code, self-reported	aortic stenosis
Atrial fibrillation or flutter	include	OPCS4	K57.1 Percutaneous transluminal ablation of atrioventricular node
Atrial fibrillation or flutter	include	OPCS4	K62.1 Percutaneous transluminal ablation of pulmonary vein to left atrium conducting system

Atrial fibrillation or flutter	include	OPCS4	K62.2 Percutaneous transluminal ablation of atrial wall for atrial flutter
Atrial fibrillation or flutter	include	OPCS4	K62.3 Percutaneous transluminal ablation of conducting system of heart for atrial flutter NEC
Atrial fibrillation or flutter	include	OPCS4	K62.4 Percutaneous transluminal internal cardioversion NEC
Atrial fibrillation or flutter	include	OPCS4	X50.1 Direct current cardioversion
Atrial fibrillation or flutter	include	OPCS4	X50.2 External cardioversion NEC
Atrial fibrillation or flutter	include	ICD10	I48 Atrial fibrillation and flutter
Atrial fibrillation or flutter	include	ICD10	I48.0 Paroxysmal atrial fibrillation
Atrial fibrillation or flutter	include	ICD10	I48.1 Persistent atrial fibrillation
Atrial fibrillation or flutter	include	ICD10	I48.2 Chronic atrial fibrillation
Atrial fibrillation	include	ICD10	I48.3 Typical atrial flutter

or flutter			
Atrial fibrillation or flutter	include	ICD10	I48.4 Atypical atrial flutter
Atrial fibrillation or flutter	include	ICD10	I48.9 Atrial fibrillation and atrial flutter, unspecified
Atrial fibrillation or flutter	include	ICD9	4273 Atrial fibrillation and flutter
Atrial fibrillation or flutter	include	Non-cancer illness code, self-reported	atrial fibrillation
Atrial fibrillation or flutter	include	Non-cancer illness code, self-reported	atrial flutter
Atrial fibrillation or flutter	include	Operation code	cardioversion
Coronary artery	include	OPCS4	K40.1 Saphenous vein graft replacement of one

disease			coronary artery
Coronary artery disease	include	OPCS4	K40.2 Saphenous vein graft replacement of two coronary arteries
Coronary artery disease	include	OPCS4	K40.3 Saphenous vein graft replacement of three coronary arteries
Coronary artery disease	include	OPCS4	K40.4 Saphenous vein graft replacement of four or more coronary arteries
Coronary artery disease	include	OPCS4	K41.1 Autograft replacement of one coronary artery NEC
Coronary artery disease	include	OPCS4	K41.2 Autograft replacement of two coronary arteries NEC
Coronary artery disease	include	OPCS4	K41.3 Autograft replacement of three coronary arteries NEC
Coronary artery disease	include	OPCS4	K41.4 Autograft replacement of four or more coronary arteries NEC
Coronary artery disease	include	OPCS4	K45.1 Double anastomosis of mammary arteries to coronary arteries
Coronary artery disease	include	OPCS4	K45.2 Double anastomosis of thoracic arteries to coronary arteries NEC

Coronary artery disease	include	OPCS4	K45.3 Anastomosis of mammary artery to left anterior descending coronary artery
Coronary artery disease	include	OPCS4	K45.4 Anastomosis of mammary artery to coronary artery NEC
Coronary artery disease	include	OPCS4	K45.5 Anastomosis of thoracic artery to coronary artery NEC
Coronary artery disease	include	OPCS4	K49.1 Percutaneous transluminal balloon angioplasty of one coronary artery
Coronary artery disease	include	OPCS4	K49.2 Percutaneous transluminal balloon angioplasty of multiple coronary arteries
Coronary artery disease	include	OPCS4	K49.8 Other specified transluminal balloon angioplasty of coronary artery
Coronary artery disease	include	OPCS4	K49.9 Unspecified transluminal balloon angioplasty of coronary artery
Coronary artery disease	include	OPCS4	K50.2 Percutaneous transluminal coronary thrombolysis using streptokinase
Coronary artery disease	include	OPCS4	K75.1 Percutaneous transluminal balloon angioplasty and insertion of 1-2 drug-eluting stents into coronary artery

Coronary artery disease	include	OPCS4	K75.2 Percutaneous transluminal balloon angioplasty and insertion of 3 or more drug-eluting stents into coronary artery
Coronary artery disease	include	OPCS4	K75.3 Percutaneous transluminal balloon angioplasty and insertion of 1-2 stents into coronary artery
Coronary artery disease	include	OPCS4	K75.4 Percutaneous transluminal balloon angioplasty and insertion of 3 or more stents into coronary artery NEC
Coronary artery disease	include	OPCS4	K75.8 Other specified percutaneous transluminal balloon angioplasty and insertion of stent into coronary artery
Coronary artery disease	include	OPCS4	K75.9 Unspecified percutaneous transluminal balloon angioplasty and insertion of stent into coronary artery
Coronary artery disease	include	Source of myocardial infarction report	Self-reported only

Coronary artery disease	include	Source of myocardial infarction report	Hospital admission
Coronary artery disease	include	Source of myocardial infarction report	Death only
Heart failure	include	ICD10	I11.0 Hypertensive heart disease with (congestive) heart failure
Heart failure	include	ICD10	I13.0 Hypertensive heart and renal disease with (congestive) heart failure
Heart failure	include	ICD10	I13.2 Hypertensive heart and renal disease with both (congestive) heart failure and renal failure
Heart failure	include	ICD10	I25.5 Ischaemic cardiomyopathy
Heart failure	include	ICD10	I42.0 Dilated cardiomyopathy
Heart failure	include	ICD10	I42.5 Other restrictive cardiomyopathy

Heart failure	include	ICD10	I42.8 Other cardiomyopathies
Heart failure	include	ICD10	I42.9 Cardiomyopathy, unspecified
Heart failure	include	ICD10	I50 Heart failure
Heart failure	include	ICD10	I50.0 Congestive heart failure
Heart failure	include	ICD10	I50.1 Left ventricular failure
Heart failure	include	ICD10	I50.9 Heart failure, unspecified
Heart failure	include	ICD9	4254 Other primary cardiomyopathies
Heart failure	include	ICD9	4280 Congestive heart failure
Heart failure	include	ICD9	4281 Left heart failure
Heart failure	include	Non-cancer illness code, self-reported	heart failure/pulmonary odema
Heart failure	include	Non-cancer illness code, self-reported	cardiomyopathy

Heart failure	exclude	ICD10	I42.1 Obstructive hypertrophic cardiomyopathy
Heart failure	exclude	ICD10	I42.2 Other hypertrophic cardiomyopathy
Heart failure	exclude	Non-cancer illness code, self-reported	hypertrophic cardiomyopathy (hcm / hocm)
Pulmonary hypertension	include	ICD9	4160 Primary pulmonary hypertension
Pulmonary hypertension	include	ICD10	I27.0 Primary pulmonary hypertension
Pulmonary hypertension	include	ICD10	I27.2 Other secondary pulmonary hypertension
Thoracic aortic aneurysm	include	ICD10	I71.1 Thoracic aortic aneurysm, ruptured
Thoracic aortic aneurysm	include	ICD10	I71.2 Thoracic aortic aneurysm, without mention of rupture
Thoracic aortic aneurysm	include	OPCS4	K33.1 Aortic root replacement using pulmonary valve autograft with right ventricle to pulmonary

			artery valved conduit
Thoracic aortic aneurysm	include	OPCS4	K33.3 Aortic root replacement using homograft
Thoracic aortic aneurysm	include	OPCS4	K33.4 Aortic root replacement using mechanical prosthesis
Thoracic aortic aneurysm	include	OPCS4	K33.5 Aortic root replacement NEC
Thoracic aortic aneurysm	include	OPCS4	L18.1 Emergency replacement of aneurysmal segment of ascending aorta by anastomosis of aorta to aorta
Thoracic aortic aneurysm	include	OPCS4	L18.2 Emergency replacement of aneurysmal segment of thoracic aorta by anastomosis of aorta to aorta NEC
Thoracic aortic aneurysm	include	OPCS4	L19.1 Replacement of aneurysmal segment of ascending aorta by anastomosis of aorta to aorta NEC
Thoracic aortic aneurysm	include	OPCS4	L19.2 Replacement of aneurysmal segment of thoracic aorta by anastomosis of aorta to aorta NEC

Thoracic aortic aneurysm	include	OPCS4	L20.1 Emergency bypass of segment of ascending aorta by anastomosis of aorta to aorta NEC
Thoracic aortic aneurysm	include	OPCS4	L21.1 Bypass of segment of ascending aorta by anastomosis of aorta to aorta NEC
Thoracic aortic aneurysm	include	OPCS4	L27.3 Endovascular insertion of stent graft for thoracic aortic aneurysm
Thoracic aortic aneurysm	include	OPCS4	L28.3 Endovascular insertion of stent for thoracic aortic aneurysm

Supplemental Table 2: Significant Associations

Trait	SNP	CHR	BP	Effect/ Non-effect allele	Closest gene	P	Previous work
Aorta 5	rs824510	2	19725556	G/A	OSR1	1.14E-13	Pirruccello et al.
Aorta 5	rs369488034	3	58129020	GA/G	FLNB	2.88E-08	Pirruccello et al.
Aorta 5	rs67846163	4	174656889	A/G	HAND2	3.01E-09	Pirruccello et al.
Aorta 5	rs4635954	5	95607323	T/G	PCSK1	5.88E-13	Pirruccello et al.
Aorta 5	rs5880559	6	143593003	A/AG	AIG1	9.31E-10	Pirruccello et al.

Aorta 5	rs6460069	7	73430120	A/T	ELN	4.80E-17	Pirruccello et al.
Aorta 5	rs11618858	13	22869283	T/C	FGF9	4.63E-11	Pirruccello et al.
Aorta 5	rs62053262	16	69969299	C/G	WWP2	1.17E-11	Pirruccello et al.
Aorta 4	rs1863777	2	19729131	T/C	OSR1	1.73E-24	Pirruccello et al.
Aorta 4	rs35930173	2	164924332	G/A	FIGN	3.48E-08	Pirruccello et al.
Aorta 4	3:58133803_AT_A	3	58133803	AT/A	FLNB	1.86E-11	Pirruccello et al.
Aorta 4	rs34266187	3	123975301	G/A	KALRN	1.25E-09	novel

Aorta 4	rs55914222	3	128202943	G/C	GATA2	2.22E-12	Pirruccello et al.
Aorta 4	4:81170475_CT_C	4	81170475	CT/C	FGF5	2.74E-08	Pirruccello et al.
Aorta 4	rs67846163	4	174656889	A/G	HAND2	4.11E-14	Pirruccello et al.
Aorta 4	rs4077816	5	95582494	A/G	PCSK1	9.48E-24	Pirruccello et al.
Aorta 4	rs335196	5	122520531	G/A	PRDM6	8.21E-10	Pirruccello et al.
Aorta 4	rs1630736	6	12295987	C/T	EDN1	1.99E-10	Pirruccello et al.
Aorta 4	rs1570350	6	143592386	A/G	AIG1	9.41E-12	Pirruccello et

							al.
Aorta 4	rs79215950	7	35277067	G/A	TBX20	9.66E-12	Pirrucc ello et al.
Aorta 4	rs4717863	7	73428879	C/T	ELN	1.71E-27	Pirrucc ello et al.
Aorta 4	rs771025673	7	85045118	AT/A	SEMA3 D	6.30E-13	Pirrucc ello et al.
Aorta 4	rs16876090	8	10836359 6	G/A	ANGPT 1	1.14E-08	Pirrucc ello et al.
Aorta 4	rs34557926	8	12460715 9	C/T	KLHL38	6.25E-13	Pirrucc ello et al.
Aorta 4	rs77218185	10	96071212	T/C	PLCE1	4.15E-08	Pirrucc ello et al.
Aorta 4	rs34943800	10	11448769	C/T	VTI1A	3.48E-09	Pirrucc

			7				ello et al.
Aorta 4	rs77889556	11	17498057	G/A	ABCC8	6.51E-09	Pirrucc ello et al.
Aorta 4	rs273582	11	30890857	C/T	DCDC1	4.54E-08	Pirrucc ello et al.
Aorta 4	rs11222084	11	130273230	A/T	ADAMTS8	1.19E-09	Pirrucc ello et al.
Aorta 4	rs2307024	12	22005003	T/G	ABCC9	5.00E-10	Pirrucc ello et al.
Aorta 4	rs12869493	13	22872349	C/T	FGF9	5.34E-17	Pirrucc ello et al.
Aorta 4	rs4905134	14	94459845	A/G	ASB2	1.55E-09	Pirrucc ello et al.

Aorta 4	rs62053262	16	69969299	C/G	WWP2	4.36E-19	Pirruccello et al.
Aorta 4	rs112648265	16	88990551	T/TG	CBFA2T3	3.64E-11	Pirruccello et al.
Aorta 4	rs7213756	17	2098339	C/A	SMG6	8.30E-14	Pirruccello et al.
Aorta 4	rs7215383	17	12182246	A/G	MAP2K4	9.34E-10	Pirruccello et al.
Aorta 4	rs4821942	22	40718100	G/A	TNRC6B	7.36E-11	Pirruccello et al.
Aorta 3	rs17535443	1	59646056	G/A	FGGY	1.70E-08	Pirruccello et al.
Aorta 3	rs116595383	2	19711073	C/A	OSR1	2.42E-24	Pirruccello et

							al.
Aorta 3	rs16849225	2	164906820	C/T	FIGN	3.64E-09	Pirruccello et al.
Aorta 3	rs12052878	2	238227594	G/A	COL6A3	1.22E-10	Pirruccello et al.
Aorta 3	rs5848609	3	41802815	G/GTTA	ULK4	6.49E-09	Pirruccello et al.
Aorta 3	rs11710658	3	58147888	G/A	FLNB	8.63E-14	Pirruccello et al.
Aorta 3	rs62270945	3	128201889	C/T	GATA2	1.78E-09	Pirruccello et al.
Aorta 3	rs67846163	4	174656889	A/G	HAND2	8.58E-13	Pirruccello et al.
Aorta 3	rs764443335	5	95606712	AATG	PCSK1	7.97E-29	Pirrucc

				/A			ello et al.
Aorta 3	rs17470137	5	122531347	G/A	PRDM6	2.48E-15	Pirrucello et al.
Aorta 3	rs496236	6	11641601	A/G	TMEM170B	1.26E-08	Pirrucello et al.
Aorta 3	rs1630736	6	12295987	C/T	EDN1	5.94E-12	Pirrucello et al.
Aorta 3	rs9470366	6	36625562	G/A	CDKN1A	2.43E-09	Pirrucello et al.
Aorta 3	rs6907215	6	143608968	C/T	AIG1	2.37E-12	Pirrucello et al.
Aorta 3	rs1362207	7	35282435	T/A	TBX20	2.42E-11	Pirrucello et al.

Aorta 3	rs6943980	7	73424373	A/C	ELN	7.04E-49	Pirruccello et al.
Aorta 3	rs1583081	7	85034227	G/T	SEMA3D	2.87E-18	Pirruccello et al.
Aorta 3	rs7845785	8	108294144	C/T	ANGPT1	3.34E-10	Pirruccello et al.
Aorta 3	rs7006122	8	124608614	T/G	KLHL38	1.46E-13	Pirruccello et al.
Aorta 3	rs71463528	10	65344190	T/TAAA	REEP3	7.34E-09	Pirruccello et al.
Aorta 3	rs12785061	10	96264077	T/C	TBC1D12	4.34E-10	Pirruccello et al.
Aorta 3	rs55646508	11	69819638	C/T	ANO1	3.14E-11	Pirruccello et

							al.
Aorta 3	rs2307024	12	22005003	T/G	ABCC9	1.31E-11	Pirrucc ello et al.
Aorta 3	rs1507721	13	22884524	C/T	FGF9	3.19E-23	Pirrucc ello et al.
Aorta 3	rs4905134	14	94459845	A/G	ASB2	1.26E-08	Pirrucc ello et al.
Aorta 3	rs11853359	15	71621524	G/A	THSD4	2.41E-10	Pirrucc ello et al.
Aorta 3	rs12708958	16	56089862	C/T	CES5A	1.78E-08	Pirrucc ello et al.
Aorta 3	rs62053262	16	69969299	C/G	WWP2	8.80E-25	Pirrucc ello et al.
Aorta 3	rs533679	16	88991500	A/G	CBFA2	9.36E-13	Pirrucc

					T3		ello et al.
Aorta 3	rs1532292	17	2097483	T/G	SMG6	1.04E-16	Pirrucc ello et al.
Aorta 3	rs4791495	17	12190157	G/A	MAP2K 4	2.42E-14	Pirrucc ello et al.
Aorta 3	rs3063286	20	10488552	T/TTA	SLX4IP	1.23E-08	Pirrucc ello et al.
Aorta 2	rs17535443	1	59646056	G/A	FGGY	4.44E-08	Pirrucc ello et al.
Aorta 2	rs824510	2	19725556	G/A	OSR1	1.86E-21	Pirrucc ello et al.
Aorta 2	rs760787102	2	164891213	ATATT/A	FIGN	9.53E-11	Pirrucc ello et al.

Aorta 2	rs12052878	2	238227594	G/A	COL6A3	9.92E-12	Pirruccello et al.
Aorta 2	rs73028182	3	14863636	A/G	FGD5	1.53E-11	Pirruccello et al.
Aorta 2	rs6794074	3	41751147	A/G	ULK4	1.51E-10	Pirruccello et al.
Aorta 2	rs13095822	3	58131979	C/T	FLNB	4.72E-15	Pirruccello et al.
Aorta 2	rs2306272	3	66434643	T/C	SLC25A26	2.76E-08	Pirruccello et al.
Aorta 2	rs62270945	3	128201889	C/T	GATA2	2.51E-11	Pirruccello et al.
Aorta 2	rs67846163	4	174656889	A/G	HAND2	5.65E-13	Pirruccello et

							al.
Aorta 2	rs540082300	5	51196504	C/CT	ISL1	2.83E-08	novel
Aorta 2	rs55745974	5	95566562	A/T	PCSK1	9.34E-42	Pirruccello et al.
Aorta 2	rs17470137	5	122531347	G/A	PRDM6	9.89E-18	Pirruccello et al.
Aorta 2	5:173276788_AT_A	5	173276788	AT/A	CPEB4	8.21E-10	novel
Aorta 2	rs496236	6	11641601	A/G	TMEM170B	1.23E-09	Pirruccello et al.
Aorta 2	rs1630736	6	12295987	C/T	EDN1	9.59E-16	Pirruccello et al.
Aorta 2	rs12199346	6	36641546	C/A	CDKN1A	7.14E-09	Pirruccello et al.

Aorta 2	rs12195791	6	72205132	G/A	OGFRL1	7.64E-09	novel
Aorta 2	rs1570350	6	143592386	A/G	AIG1	2.50E-13	Pirruccello et al.
Aorta 2	rs13203975	6	152333104	G/A	ESR1	3.88E-11	Pirruccello et al.
Aorta 2	rs79215950	7	35277067	G/A	TBX20	1.44E-12	Pirruccello et al.
Aorta 2	rs6974735	7	73428222	A/G	ELN	4.24E-46	Pirruccello et al.
Aorta 2	rs771025673	7	85045118	AT/A	SEMA3D	1.98E-22	Pirruccello et al.
Aorta 2	8:122634926_CA_C	8	122634926	CA/C	HAS2	1.62E-11	Pirruccello et al.

Aorta 2	rs6470156	8	124579985	G/A	FBXO32	4.72E-14	Pirruccello et al.
Aorta 2	rs10995020	10	63816077	C/G	ARID5B	2.76E-09	Pirruccello et al.
Aorta 2	rs77218185	10	96071212	T/C	PLCE1	5.95E-14	Pirruccello et al.
Aorta 2	rs146473682	11	30875859	CT/C	DCDC1	3.92E-09	Pirruccello et al.
Aorta 2	rs55646508	11	69819638	C/T	ANO1	1.30E-11	Pirruccello et al.
Aorta 2	rs2307024	12	22005003	T/G	ABCC9	1.52E-13	Pirruccello et al.
Aorta 2	rs56298756	12	62777565	G/T	USP15	6.28E-10	Pirruccello et

							al.
Aorta 2	rs2137537	12	71113087	T/C	PTPRR	8.19E-12	novel
Aorta 2	rs9506822	13	22862220	A/G	FGF9	9.39E-36	Pirrucc ello et al.
Aorta 2	rs2740515	13	50760310	G/C	DLEU1	4.21E-08	Pirrucc ello et al.
Aorta 2	rs1848050	15	48862043	G/A	FBN1	5.56E-10	Pirrucc ello et al.
Aorta 2	rs6494904	15	71609522	G/A	THSD4	5.62E-15	Pirrucc ello et al.
Aorta 2	16:56221642 _AAAT_A	16	56221642	AAAT /A	GNAO1	1.25E-09	Pirrucc ello et al.
Aorta 2	rs62053262	16	69969299	C/G	WWP2	3.55E-22	Pirrucc ello et al.

Aorta 2	rs7500448	16	83045790	A/G	CDH13	1.23E-12	Pirrucc ello et al.
Aorta 2	rs11862605	16	89029267	A/G	CBFA2 T3	4.84E-15	Pirrucc ello et al.
Aorta 2	rs7213756	17	2098339	C/A	SMG6	6.78E-20	Pirrucc ello et al.
Aorta 2	rs7221449	17	12191884	C/T	MAP2K 4	3.93E-18	Pirrucc ello et al.
Aorta 2	rs3063286	20	10488552	T/TTA	SLX4IP	6.50E-11	Pirrucc ello et al.
Aorta 2	rs147036721	22	40547564	G/GA AAA	TNRC6 B	9.34E-09	Pirrucc ello et al.
Aorta 1	rs747347287	1	45418228	AT/A	EIF2B3	7.73E-09	novel
Aorta 1	rs824510	2	19725556	G/A	OSR1	6.73E-23	Pirrucc

							ello et al.
Aorta 1	rs760787102	2	164891213	ATATT/A	FIGN	4.75E-12	Pirruccello et al.
Aorta 1	rs12052878	2	238227594	G/A	COL6A3	3.78E-11	Pirruccello et al.
Aorta 1	rs73028182	3	14863636	A/G	FGD5	1.03E-10	Pirruccello et al.
Aorta 1	rs5848609	3	41802815	G/GTTA	ULK4	5.31E-09	Pirruccello et al.
Aorta 1	3:58133803_AT_A	3	58133803	AT/A	FLNB	4.27E-15	Pirruccello et al.
Aorta 1	rs2306272	3	66434643	T/C	SLC25A26	3.25E-08	Pirruccello et al.

Aorta 1	rs62270945	3	128201889	C/T	GATA2	9.71E-09	Pirruccello et al.
Aorta 1	rs1979974	4	146800815	A/G	ZNF827	9.39E-09	novel
Aorta 1	rs67846163	4	174656889	A/G	HAND2	1.05E-08	Pirruccello et al.
Aorta 1	rs13158444	5	51201361	T/C	ISL1	2.95E-09	novel
Aorta 1	rs55745974	5	95566562	A/T	PCSK1	2.48E-33	Pirruccello et al.
Aorta 1	rs335196	5	122520531	G/A	PRDM6	9.21E-21	Pirruccello et al.
Aorta 1	rs62376928	5	173288146	T/C	CPEB4	2.67E-10	novel
Aorta 1	rs2070699	6	12292772	G/T	EDN1	7.28E-14	Pirruccello et al.

Aorta 1	rs143917622	6	72205158	A/AT	OGFRL 1	7.80E-09	novel
Aorta 1	rs6941056	6	14359182 1	C/G	AIG1	2.58E-08	Pirrucc ello et al.
Aorta 1	rs2207231	6	15232988 4	A/G	ESR1	3.84E-11	Pirrucc ello et al.
Aorta 1	rs6974735	7	73428222	A/G	ELN	2.94E-41	Pirrucc ello et al.
Aorta 1	rs771025673	7	85045118	AT/A	SEMA3 D	3.08E-11	Pirrucc ello et al.
Aorta 1	rs112621658	8	38774696	C/A	PLEKH A2	4.70E-10	novel
Aorta 1	rs9721183	8	75781818	C/T	PI15	3.63E-08	Pirrucc ello et al.
Aorta 1	rs10089014	8	12263576	C/T	HAS2	5.99E-11	Pirrucc

			7				ello et al.
Aorta 1	rs6470156	8	124579985	G/A	FBXO32	2.89E-11	Pirruccello et al.
Aorta 1	rs40430	10	79179345	A/T	KCNMA1	1.88E-10	novel
Aorta 1	rs1343094	10	95900635	T/A	PLCE1	1.29E-14	Pirruccello et al.
Aorta 1	rs146473682	11	30875859	CT/C	DCDC1	8.65E-10	Pirruccello et al.
Aorta 1	rs55646508	11	69819638	C/T	ANO1	5.15E-12	Pirruccello et al.
Aorta 1	rs11222084	11	130273230	A/T	ADAMTS8	1.36E-11	Pirruccello et al.
Aorta 1	rs10743356	12	20235039	A/G	PDE3A	2.92E-11	novel

Aorta 1	rs2307024	12	22005003	T/G	ABCC9	1.21E-14	Pirruccello et al.
Aorta 1	rs7304603	12	71114400	T/C	PTPRR	3.78E-13	novel
Aorta 1	rs4144503	12	94141772	T/A	CRADD	3.83E-08	Pirruccello et al.
Aorta 1	rs7994761	13	22871446	A/G	FGF9	1.14E-30	Pirruccello et al.
Aorta 1	rs2740515	13	50760310	G/C	DLEU1	2.24E-09	Pirruccello et al.
Aorta 1	rs1848050	15	48862043	G/A	FBN1	3.12E-16	Pirruccello et al.
Aorta 1	rs1441358	15	71612514	T/G	THSD4	6.02E-14	Pirruccello et al.
Aorta 1	16:14505488	16	14505488	CT/C	PARN	1.36E-09	novel

	_CT_C						
Aorta 1	rs62053262	16	69969299	C/G	WWP2	4.16E-12	Pirruccello et al.
Aorta 1	rs7500448	16	83045790	A/G	CDH13	3.95E-15	Pirruccello et al.
Aorta 1	rs488327	16	88989005	T/C	CBFA2T3	3.95E-11	Pirruccello et al.
Aorta 1	rs1002135	17	2097583	T/G	SMG6	4.34E-26	Pirruccello et al.
Aorta 1	rs7221449	17	12191884	C/T	MAP2K4	7.08E-15	Pirruccello et al.
Aorta 1	rs35296742	17	40999303	G/A	AOC2	4.41E-08	novel
Aorta 1	rs264282	18	10917258	A/G	PIEZO2	8.01E-09	Pirruccello et al.

Aorta 1	rs3063286	20	10488552	T/TTA	SLX4IP	9.05E-12	Pirruccello et al.
Aorta 1	rs6035357	20	19478696	C/T	SLC24A3	7.18E-10	Pirruccello et al.
Aorta 1	rs4821942	22	40718100	G/A	TNRC6B	2.30E-09	Pirruccello et al.
Aorta 0	rs824510	2	19725556	G/A	OSR1	2.17E-22	Pirruccello et al.
Aorta 0	rs9869210	3	58130276	G/C	FLNB	1.63E-10	Pirruccello et al.
Aorta 0	rs188848834	4	174681501	C/T	HAND2	4.91E-10	Pirruccello et al.
Aorta 0	rs764443335	5	95606712	AATG/A	PCSK1	7.83E-19	Pirruccello et

							al.
Aorta 0	rs7734507	5	122605896	C/T	CEP120	2.11E-17	Pirruccello et al.
Aorta 0	rs2070699	6	12292772	G/T	EDN1	1.09E-11	Pirruccello et al.
Aorta 0	6:152379347_TA_T	6	152379347	TA/T	ESR1	3.56E-10	Pirruccello et al.
Aorta 0	rs917275	7	28658522	A/G	CREB5	2.91E-08	novel
Aorta 0	rs4717863	7	73428879	C/T	ELN	4.99E-22	Pirruccello et al.
Aorta 0	rs112621658	8	38774696	C/A	PLEKHA2	5.52E-10	novel
Aorta 0	rs40430	10	79179345	A/T	KCNMA1	4.34E-10	novel
Aorta 0	rs1343094	10	95900635	T/A	PLCE1	1.03E-11	Pirrucc

							ello et al.
Aorta 0	rs112807178	11	69822783	G/A	ANO1	1.40E-12	Pirrucc ello et al.
Aorta 0	rs11222084	11	130273230	A/T	ADAMTS8	1.25E-10	Pirrucc ello et al.
Aorta 0	rs10841441	12	20210632	C/T	PDE3A	4.54E-17	novel
Aorta 0	rs861202	12	21994955	G/C	ABCC9	5.13E-11	Pirrucc ello et al.
Aorta 0	rs2137537	12	71113087	T/C	PTPRR	1.57E-10	novel
Aorta 0	rs35715048	12	94200555	G/A	CRADD	1.16E-08	Pirrucc ello et al.
Aorta 0	rs9316871	13	22861921	A/G	FGF9	7.99E-19	Pirrucc ello et al.

Aorta 0	rs2687939	13	50760323	A/G	DLEU1	1.43E-11	Pirruccello et al.
Aorta 0	rs1036477	15	48914926	A/G	FBN1	4.09E-12	Pirruccello et al.
Aorta 0	rs6494904	15	71609522	G/A	THSD4	1.51E-08	Pirruccello et al.
Aorta 0	rs7500448	16	83045790	A/G	CDH13	6.87E-11	Pirruccello et al.
Aorta 0	rs1532292	17	2097483	T/G	SMG6	3.81E-26	Pirruccello et al.
Aorta 0	rs7221449	17	12191884	C/T	MAP2K4	6.07E-10	Pirruccello et al.
Aorta 0	rs78033733	17	45290078	T/G	MYL4	8.66E-09	novel
Aorta 0	rs57785785	19	58815158	T/A	ZNF8	1.08E-08	novel

Aorta 0	rs147036721	22	40547564	G/GAAAA	TNRC6B	7.67E-09	Pirruccello et al.
Aortic root	rs76947392	1	1256608	G/A	CPSF3L	2.19E-08	novel
Aortic root	rs12733512	1	59646978	C/T	FGGY	4.02E-10	Wild et al.
Aortic root	1:100033312_TA_T	1	100033312	TA/T	PALMD	8.96E-25	Wild et al.
Aortic root	rs1285677	1	232712355	A/C	SIPA1L2	7.20E-13	novel
Aortic root	rs2686630	3	58091861	G/C	FLNB	3.20E-09	novel
Aortic root	rs73030346	3	169317856	C/T	MECOM	3.54E-08	novel
Aortic root	rs13134800	4	120900282	T/C	MAD2L1	4.61E-10	novel
Aortic root	5:15005465_CTCTT_C	5	15005465	CTCTT/C	ANKH	2.68E-08	novel

Aortic root	rs4264961	5	95617018	C/T	PCSK1	3.15E-10	novel
Aortic root	rs77097530	5	122609853	C/G	CEP120	1.99E-12	Wild et al.
Aortic root	rs1630736	6	12295987	C/T	EDN1	9.69E-11	novel
Aortic root	rs80036911	6	16472975	C/T	ATXN1	1.63E-08	novel
Aortic root	rs7754762	6	152311537	T/A	ESR1	3.06E-09	novel
Aortic root	rs28735	10	79178044	G/C	KCNMA1	2.80E-11	novel
Aortic root	rs1977289	10	96301907	T/C	HELLS	2.63E-10	novel
Aortic root	rs72931748	11	69825414	A/G	ANO1	1.14E-11	Wild et al.
Aortic root	rs12280388	11	121670712	T/C	SORL1	2.48E-12	novel
Aortic	rs4765663	12	2178760	G/C	CACNA	3.79E-08	Wild et

root					1C		al.
Aortic root	rs10770612	12	20230639	A/G	PDE3A	5.71E-25	Wild et al.
Aortic root	rs4296081	12	22005781	A/G	ABCC9	1.94E-10	novel
Aortic root	12:66404136_AAAAC_A	12	66404136	AAAAC/A	HMGA2	6.99E-13	Wild et al.
Aortic root	rs903175	12	94158719	G/A	CRADD	2.73E-10	novel
Aortic root	rs12866004	13	22865917	T/A	FGF9	5.20E-16	novel
Aortic root	rs2740515	13	50760310	G/C	DLEU1	9.97E-28	Wild et al.
Aortic root	rs17352842	15	48694211	C/T	FBN1	1.93E-08	novel
Aortic root	rs139939693	15	63859576	C/T	USP3	3.40E-10	Wild et al.
Aortic root	rs1002135	17	2097583	T/G	SMG6	1.61E-20	Wild et al.

Aortic root	rs17677363	17	45036112	A/T	GOSR2	2.99E-22	Wild et al.
LVOT	rs35631249	4	73443865	C/A	ADAMTS3	3.28E-08	novel
LVOT	rs7139226	12	20180749	C/T	AEBP2	9.36E-11	novel
LVOT	rs10400419	12	66389968	T/C	HMGA2	7.77E-10	novel
LVOT	rs2740516	13	50761619	G/A	DLEU1	2.27E-09	novel
LVOT	rs17677363	17	45036112	A/T	GOSR2	4.11E-19	novel
LVOT	rs62240962	22	42259524	C/T	SREBF2	9.75E-09	novel

Supplemental Table 3: Post-QC phenotype counts

Diameter	**n**
Aorta 5	19300
Aorta 4	27102
Aorta 3	32259
Aorta 2	33870
Aorta 1	33866
Aorta 0	33857
Aortic root	33868
LVOT	33870

Supplemental Table 4: Phenotype SNP counts

Trait	SNPs
LVOT	11247266
Aortic root	11247266
Aorta 0	11247285
Aorta 1	11247281
Aorta 2	11247266
Aorta 3	11245622
Aorta 4	11241047
Aorta 5	11241373

Supplemental Table 5: Location of phenotypes

Phenotype name	Description
Aorta 5	Diameter of the ascending aorta, 53mm distal to the sinotubular junction for a patient of mean height
Aorta 4	Diameter of the ascending aorta, 43mm distal to the sinotubular junction for a patient of mean height
Aorta 3	Diameter of the ascending aorta, 33mm distal to the sinotubular junction for a patient of mean height
Aorta 2	Diameter of the ascending aorta, 23mm distal to the sinotubular junction for a patient of mean height
Aorta 1	Diameter of the ascending aorta, 13mm distal to the sinotubular junction for a patient of mean height
Aorta 0	Diameter of the ascending aorta, 3mm distal to the sinotubular junction for a patient of mean height
Aortic root	Diameter of ascending aorta at the level of the sinuses of Valsalva
LVOT	Diameter of the left ventricular outflow tract

Supplemental Table 6: Prediction of Disease

Prevalent disease	Diameter (scaled)	N (disease)	Beta	SE	P
Thoracic aortic aneurysm	Aorta 5	12	1.934	0.316	9.56E-10
Thoracic aortic aneurysm	Aorta 4	12	2.293	0.301	2.82E-14
Thoracic aortic aneurysm	Aorta 3	12	2.538	0.288	1.44E-18
Thoracic aortic aneurysm	Aorta 2	12	2.774	0.288	7.08E-22
Thoracic aortic aneurysm	Aorta 1	12	2.556	0.288	8.28E-19
Thoracic aortic aneurysm	Aorta 0	12	2.076	0.289	6.38E-13
Thoracic aortic aneurysm	Aortic root	12	2.057	0.289	1.02E-12
Thoracic aortic aneurysm	LVOT	12	2.000	0.289	4.24E-12
Aortic stenosis	Aorta 5	99	0.593	0.123	1.53E-06
Aortic stenosis	Aorta 4	99	0.558	0.108	2.37E-07
Aortic stenosis	Aorta 3	99	0.474	0.102	3.56E-06

Aortic stenosis	Aorta 2	99	0.556	0.101	3.28E-08
Aortic stenosis	Aorta 1	99	0.433	0.101	1.83E-05
Aortic stenosis	Aorta 0	99	0.244	0.101	0.015
Aortic stenosis	Aortic root	99	0.232	0.101	0.021
Aortic stenosis	LVOT	99	0.321	0.101	0.001

Supplemental Table 7: Correlations between diameters and their polygenic scores

Trait	PRS-Diameter correlation (Pearson's r)
LVOT	0.72
Aortic root	0.72
Aorta 0	0.75
Aorta 1	0.75
Aorta 2	0.76
Aorta 3	0.77
Aorta 4	0.79
Aorta 5	0.84

Supplemental Table 8: SNPs in Figure 2A and Supplemental Figure 4

Label in figure	Closest gene	SNP
ABCC8	ABCC8	rs77889556
ABCC9 1	ABCC9	rs4296081
ABCC9 2	ABCC9	rs861202
ABCC9 3	ABCC9	rs2307024
ADAMTS3	ADAMTS3	rs35631249
ADAMTS8	ADAMTS8	rs11222084
AEBP2	AEBP2	rs7139226
AIG1 1	AIG1	rs6941056
AIG1 2	AIG1	rs1570350
AIG1 3	AIG1	rs6907215
AIG1 4	AIG1	rs5880559
ANGPT1 1	ANGPT1	rs7845785
ANGPT1 2	ANGPT1	rs16876090
ANKH	ANKH	5:15005465_CTCTT_C
ANO1 1	ANO1	rs72931748
ANO1 2	ANO1	rs112807178
ANO1 3	ANO1	rs55646508

AOC2	AOC2	rs35296742
ARID5B	ARID5B	rs10995020
ASB2	ASB2	rs4905134
ATXN1	ATXN1	rs80036911
CACNA1C	CACNA1C	rs4765663
CBFA2T3 1	CBFA2T3	rs488327
CBFA2T3 2	CBFA2T3	rs11862605
CBFA2T3 3	CBFA2T3	rs533679
CBFA2T3 4	CBFA2T3	rs112648265
CDH13	CDH13	rs7500448
CDKN1A 1	CDKN1A	rs12199346
CDKN1A 2	CDKN1A	rs9470366
CEP120 1	CEP120	rs77097530
CEP120 2	CEP120	rs7734507
CES5A	CES5A	rs12708958
COL6A3	COL6A3	rs12052878
CPEB4 1	CPEB4	rs62376928
CPEB4 2	CPEB4	5:173276788_AT_A
CPSF3L	CPSF3L	rs76947392

CRADD 1	CRADD	rs903175
CRADD 2	CRADD	rs35715048
CRADD 3	CRADD	rs4144503
CREB5	CREB5	rs917275
DCDC1 1	DCDC1	rs146473682
DCDC1 2	DCDC1	rs273582
DLEU1 1	DLEU1	rs2740515
DLEU1 2	DLEU1	rs2687939
DLEU1 3	DLEU1	rs2740516
EDN1 1	EDN1	rs1630736
EDN1 2	EDN1	rs2070699
EIF2B3	EIF2B3	rs747347287
ELN 1	ELN	rs4717863
ELN 2	ELN	rs6974735
ELN 3	ELN	rs6943980
ELN 4	ELN	rs6460069
ESR1 1	ESR1	rs7754762
ESR1 2	ESR1	6:152379347_TA_T
ESR1 3	ESR1	rs2207231

ESR1 4	ESR1	rs13203975
FBN1 1	FBN1	rs17352842
FBN1 2	FBN1	rs1036477
FBN1 3	FBN1	rs1848050
FBXO32	FBXO32	rs6470156
FGD5	FGD5	rs73028182
FGF5	FGF5	4:81170475_CT_C
FGF9 1	FGF9	rs12866004
FGF9 2	FGF9	rs9316871
FGF9 3	FGF9	rs7994761
FGF9 4	FGF9	rs9506822
FGF9 5	FGF9	rs1507721
FGF9 6	FGF9	rs12869493
FGF9 7	FGF9	rs11618858
FGGY 1	FGGY	rs12733512
FGGY 2	FGGY	rs17535443
FIGN 1	FIGN	rs760787102
FIGN 2	FIGN	rs16849225
FIGN 3	FIGN	rs35930173

FLNB 1	FLNB	rs2686630
FLNB 2	FLNB	rs9869210
FLNB 3	FLNB	3:58133803_AT_A
FLNB 4	FLNB	rs13095822
FLNB 5	FLNB	rs11710658
FLNB 6	FLNB	rs369488034
GATA2 1	GATA2	rs62270945
GATA2 2	GATA2	rs55914222
GNAO1	GNAO1	16:56221642_AAAT_A
GOSR2	GOSR2	rs17677363
HAND2 1	HAND2	rs188848834
HAND2 2	HAND2	rs67846163
HAS2 1	HAS2	rs10089014
HAS2 2	HAS2	8:122634926_CA_C
HELLS	HELLS	rs1977289
HMGA2 1	HMGA2	12:66404136_AAAAC_A

HMGA2 2	HMGA2	rs10400419
ISL1 1	ISL1	rs13158444
ISL1 2	ISL1	rs540082300
KALRN	KALRN	rs34266187
KCNMA1 1	KCNMA1	rs28735
KCNMA1 2	KCNMA1	rs40430
KLHL38 1	KLHL38	rs7006122
KLHL38 2	KLHL38	rs34557926
MAD2L1	MAD2L1	rs13134800
MAP2K4 1	MAP2K4	rs7221449
MAP2K4 2	MAP2K4	rs4791495
MAP2K4 3	MAP2K4	rs7215383
MECOM	MECOM	rs73030346
MYL4	MYL4	rs78033733
OGFRL1 1	OGFRL1	rs143917622
OGFRL1 2	OGFRL1	rs12195791
OSR1 1	OSR1	rs824510
OSR1 2	OSR1	rs116595383
OSR1 3	OSR1	rs1863777

PALMD	PALMD	1:100033312_TA_T
PARN	PARN	16:14505488_CT_C
PCSK1 1	PCSK1	rs4264961
PCSK1 2	PCSK1	rs764443335
PCSK1 3	PCSK1	rs55745974
PCSK1 4	PCSK1	rs4077816
PCSK1 5	PCSK1	rs4635954
PDE3A 1	PDE3A	rs10770612
PDE3A 2	PDE3A	rs10841441
PDE3A 3	PDE3A	rs10743356
PI15	PI15	rs9721183
PIEZO2	PIEZO2	rs264282
PLCE1 1	PLCE1	rs1343094
PLCE1 2	PLCE1	rs77218185
PLEKHA2	PLEKHA2	rs112621658
PRDM6 1	PRDM6	rs335196
PRDM6 2	PRDM6	rs17470137
PTPRR 1	PTPRR	rs2137537

PTPRR 2	PTPRR	rs7304603
REEP3	REEP3	rs71463528
SEMA3D 1	SEMA3D	rs771025673
SEMA3D 2	SEMA3D	rs1583081
SIPA1L2	SIPA1L2	rs1285677
SLC24A3	SLC24A3	rs6035357
SLC25A26	SLC25A26	rs2306272
SLX4IP	SLX4IP	rs3063286
SMG6 1	SMG6	rs1002135
SMG6 2	SMG6	rs1532292
SMG6 3	SMG6	rs7213756
SORL1	SORL1	rs12280388
SREBF2	SREBF2	rs62240962
TBC1D12	TBC1D12	rs12785061
TBX20 1	TBX20	rs79215950
TBX20 2	TBX20	rs1362207
THSD4 1	THSD4	rs6494904
THSD4 2	THSD4	rs1441358
THSD4 3	THSD4	rs11853359
TMEM170B	TMEM170B	rs496236

TNRC6B 1	TNRC6B	rs147036721
TNRC6B 2	TNRC6B	rs4821942
ULK4 1	ULK4	rs5848609
ULK4 2	ULK4	rs6794074
USP15	USP15	rs56298756
USP3	USP3	rs139939693
VTI1A	VTI1A	rs34943800
WWP2	WWP2	rs62053262
ZNF8	ZNF8	rs57785785
ZNF827	ZNF827	rs1979974

Supplemental Table 9: SNP heritability of traits

Trait	SNP heritability	SE	95% CI min	95% CI max
LVOT	0.22	0.02	0.18	0.25
Aortic root	0.36	0.02	0.32	0.39
Aorta 0	0.37	0.02	0.33	0.4
Aorta 1	0.49	0.02	0.45	0.52
Aorta 2	0.49	0.02	0.45	0.52
Aorta 3	0.44	0.02	0.4	0.48
Aorta 4	0.45	0.02	0.4	0.49
Aorta 5	0.4	0.03	0.34	0.46

Supplemental Table 10: Results of confirmatory accelerated failure time analysis

Incident disease	Trait	N_Disease	Value	SE	P
Aortic stenosis	LVOT	3551	-4.49E-02	1.11E-02	5.13E-05
Aortic stenosis	Aortic root	3551	-5.18E-02	1.11E-02	2.93E-06
Aortic stenosis	Aorta 0	3551	-4.90E-02	1.10E-02	9.02E-06
Aortic stenosis	Aorta 1	3551	-2.97E-02	1.10E-02	7.14E-03
Aortic stenosis	Aorta 2	3551	-1.35E-02	1.10E-02	2.19E-01
Aortic stenosis	Aorta 3	3551	-2.34E-03	1.10E-02	8.31E-01
Aortic stenosis	Aorta 4	3551	2.00E-03	1.10E-02	8.56E-01
Aortic stenosis	Aorta 5	3551	5.17E-03	1.10E-02	6.38E-01
Thoracic aortic aneurysm	LVOT	743	-1.18E-01	2.45E-02	1.56E-06
Thoracic aortic aneurysm	Aortic root	743	-1.93E-01	2.51E-02	1.53E-14
Thoracic aortic aneurysm	Aorta 0	743	-2.14E-01	2.52E-02	2.20E-17
Thoracic aortic aneurysm	Aorta 1	743	-2.25E-01	2.54E-02	7.57E-19
Thoracic aortic aneurysm	Aorta 2	743	-2.03E-01	2.50E-02	4.89E-16
Thoracic aortic aneurysm	Aorta 3	743	-1.98E-01	2.49E-02	2.16E-15
Thoracic aortic aneurysm	Aorta 4	743	-1.61E-01	2.46E-02	5.58E-11
Thoracic aortic aneurysm	Aorta 5	743	-7.33E-02	2.41E-02	2.36E-03

References

1. Sudlow C, Gallacher J, Allen N, et al. UK biobank: an open access resource for identifying the causes of a wide range of complex diseases of middle and old age. PLoS Med. 2015;12:e1001779.

2. Petersen SE, Matthews PM, Bamberg F, et al. Imaging in population science: cardiovascular magnetic resonance in 100,000 participants of UK Biobank-rationale, challenges and approaches. J. Cardiovasc. Magn. Reson. 2013;15:46.

3. Petersen SE, Matthews PM, Francis JM, et al. UK Biobank's cardiovascular magnetic resonance protocol. J. Cardiovasc. Magn. Reson. 2015;18:8.

4. Pirruccello JP, Chaffin MD, Chou EL, et al. Deep learning enables genetic analysis of the human thoracic aorta. Nature Genetics 2022;54:40–51.

5. Howard J, Gugger S. Fastai: A layered API for deep learning. Information 2020;11:108.

6. Ronneberger O, Fischer P, Brox T. U-net: Convolutional networks for biomedical image segmentation. In: International Conference on Medical image computing and computer-assisted intervention. Springer, 2015:234–241.

7. Deng J, Dong W, Socher R, Li L-J, Li K, Fei-Fei L. Imagenet: A large-scale hierarchical image database. In: 2009 IEEE conference on computer vision and pattern recognition. Ieee, 2009:248–255.

8. Zhang TY, Suen CY. A fast parallel algorithm for thinning digital patterns. Commun. ACM 1984;27:236–239.

9. van der Walt S, Schönberger JL, Nunez-Iglesias J, et al. scikit-image: image processing in Python. PeerJ 2014;2:e453.

10. Bycroft C, Freeman C, Petkova D, et al. The UK Biobank resource with deep phenotyping

and genomic data. Nature 2018;562:203–209.

11. Loh P-R, Tucker G, Bulik-Sullivan BK, et al. Efficient Bayesian mixed-model analysis increases association power in large cohorts. Nat. Genet. 2015;47:284.

12. Eveborn GW, Schirmer H, Heggelund G, Lunde P, Rasmussen K. The evolving epidemiology of valvular aortic stenosis. the Tromsø study. Heart 2013;99:396–400.

13. Mbatchou J, Barnard L, Backman J, et al. Computationally efficient whole-genome regression for quantitative and binary traits. Nat. Genet. 2021;53:1097–1103.

14. Chang CC, Chow CC, Tellier LC, Vattikuti S, Purcell SM, Lee JJ. Second-generation PLINK: rising to the challenge of larger and richer datasets. Gigascience 2015;4:s13742–015.

15. Van Hout CV, Tachmazidou I, Backman JD, et al. Exome sequencing and characterization of 49,960 individuals in the UK Biobank. Nature 2020;586:749–756.

16. Regier AA, Farjoun Y, Larson DE, et al. Functional equivalence of genome sequencing analysis pipelines enables harmonized variant calling across human genetics projects. Nat. Commun. 2018;9:4038.

17. McLaren W, Gil L, Hunt SE, et al. The Ensembl Variant Effect Predictor. Genome Biol. 2016;17:122.

18. Karczewski KJ, Francioli LC, Tiao G, et al. The mutational constraint spectrum quantified from variation in 141,456 humans. Nature 2020;581:434–443.

19. Wild PS, Felix JF, Schillert A, et al. Large-scale genome-wide analysis identifies genetic variants associated with cardiac structure and function. J. Clin. Invest. 2017;127:1798–1812.

20. Machiela MJ, Chanock SJ. LDassoc: an online tool for interactively exploring genome-wide association study results and prioritizing variants for functional investigation. Bioinformatics 2018;34:887–889.

21. Ge T, Chen C-Y, Ni Y, Feng Y-CA, Smoller JW. Polygenic prediction via Bayesian regression and continuous shrinkage priors. Nat. Commun. 2019;10:1776.

22. Kent KC, Zwolak RM, Egorova NN, et al. Analysis of risk factors for abdominal aortic aneurysm in a cohort of more than 3 million individuals. J. Vasc. Surg. 2010;52:539–548.